Supplement of Atmos. Chem. Phys., 14, 7953–7993, 2014
http://www.atmos-chem-phys.net/14/7953/2014/
doi:10.5194/acp-14-7953-2014-supplement

Atmospheric Chemistry and Physics Open Access

Supplement of

Modelling non-equilibrium secondary organic aerosol formation and evaporation with the aerosol dynamics, gas- and particle-phase chemistry kinetic multilayer model ADCHAM

P. Roldin et al.

Correspondence to: P. Roldin (pontus.roldin@nuclear.lu.se)

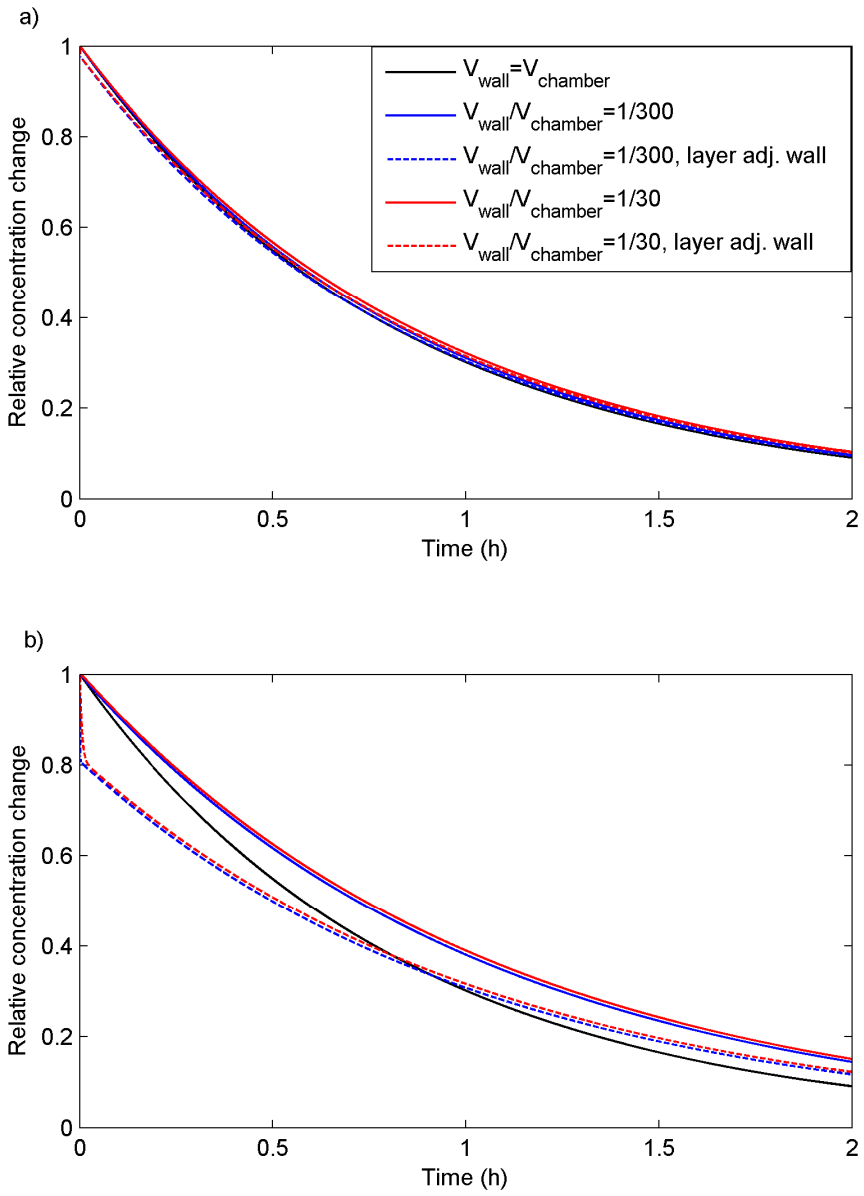

Figure S1. Example of modelled reversible gas-wall uptake onto smog chamber Teflon walls of a compound with $p_0 = 10^{-5}$ Pa and $C_w / \left(M_w \gamma_{w,i}\right) = 100$ µmol m^{-3}. The model results are for a 6 m^3 Teflon chamber with $k_{g,w} = (V_{chamber}/V_{wall}) k_{g,w}^*$ s^{-1}, $k_{g,w}^* = 1/3000$ s^{-1} . In (**a**) the model results are from simulations where $\Delta x = 1$ mm, while in (**b**) $\Delta x = 10$ mm. The relative concentration change is given both for the well mixed chamber air volume and the thin air layer adjacent to the chamber walls. If $V_{chamber}/V_{wall} = 1/300$ this layer is 1 mm thick, while if $V_{chamber}/V_{wall} = 1/30$ this layer is 10 mm thick.

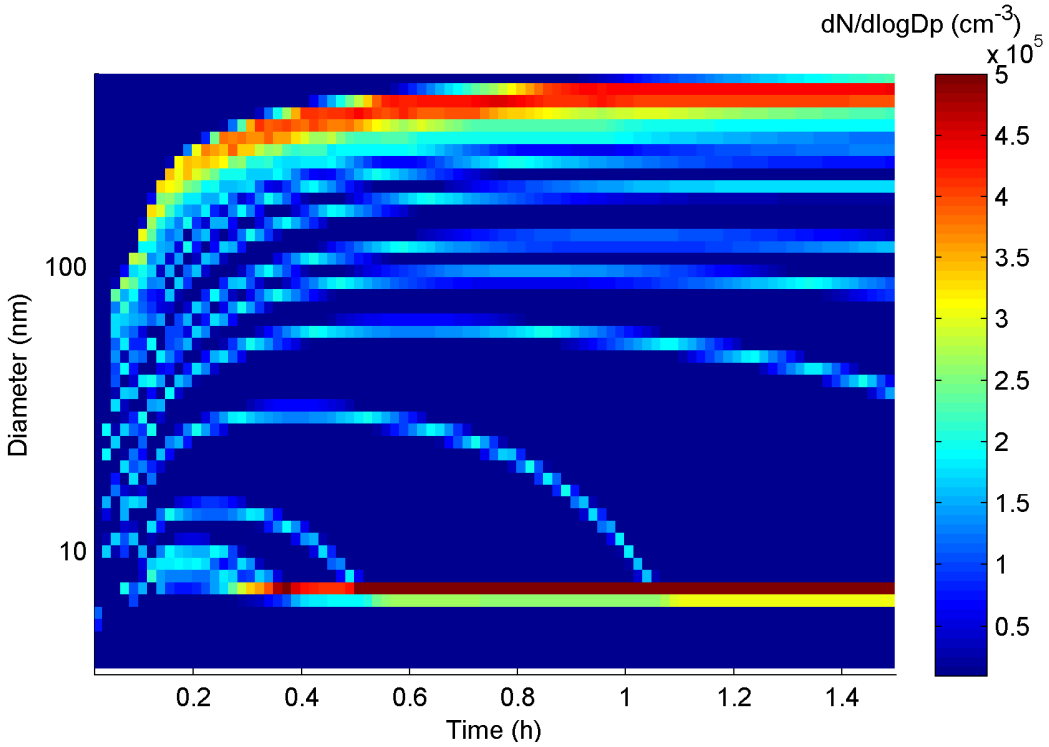

Figure S2. Modelled temporal evolution of the particle number size distribution. The results presented in this figure are from a simulation with initially 200 ppb α-pinene, 500 ppb O_3 and 250 ppm cyclohexane as OH-scavenger, semi-solid particles, no oligomerization and with pure-liquid saturation vapour pressures from the SIMPOL method. The condensational growth of the particles was modelled with the full moving method (Sect. 2.2.4). However, the particle number size distribution was converted to a fixed diameter grid for the plot.

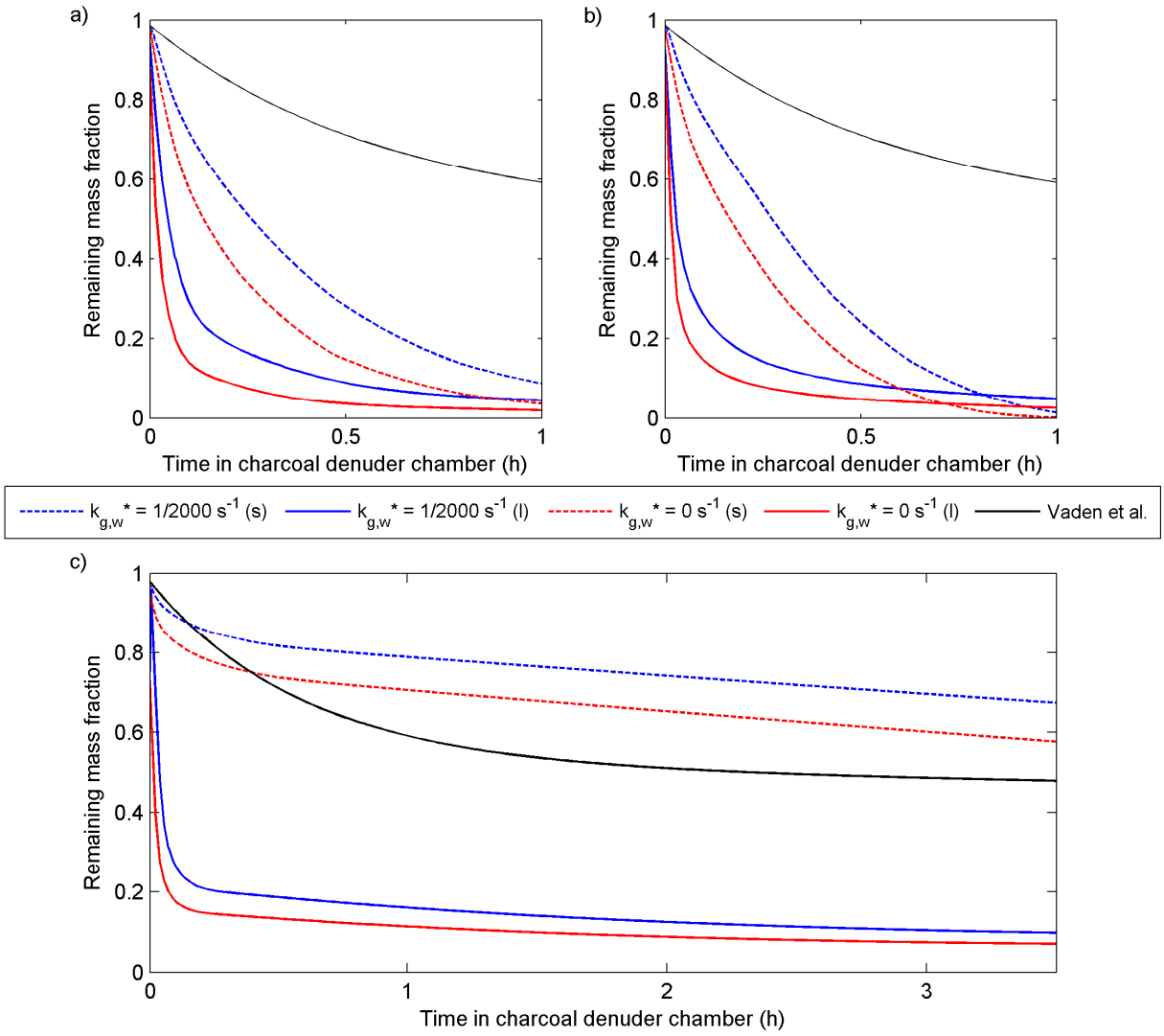

Figure S3. Modelled and measured (Vaden et al., 2011) evaporation rates of fresh α-pinene SOA, with a diameter of ~250 nm. (**a**) Model results for SOA particles with volatility according to the VBS parameterization from Pathak et al. (2007). (**b**) Model results are from simulations with MCMv3.2 and vapour pressures estimated with SIMPOL. (**c**) Model results using vapour pressures estimated with the Nannoolal method. The evaporation loss rates are given for $k_{g,w}^{*}$ = 1/2000 s^{-1} and $k_{g,w}^{*}$ = 0 s^{-1}. $C_w / \left(M_w \gamma_{w,i}\right)$ was set to 100 µmol m^{-3}.

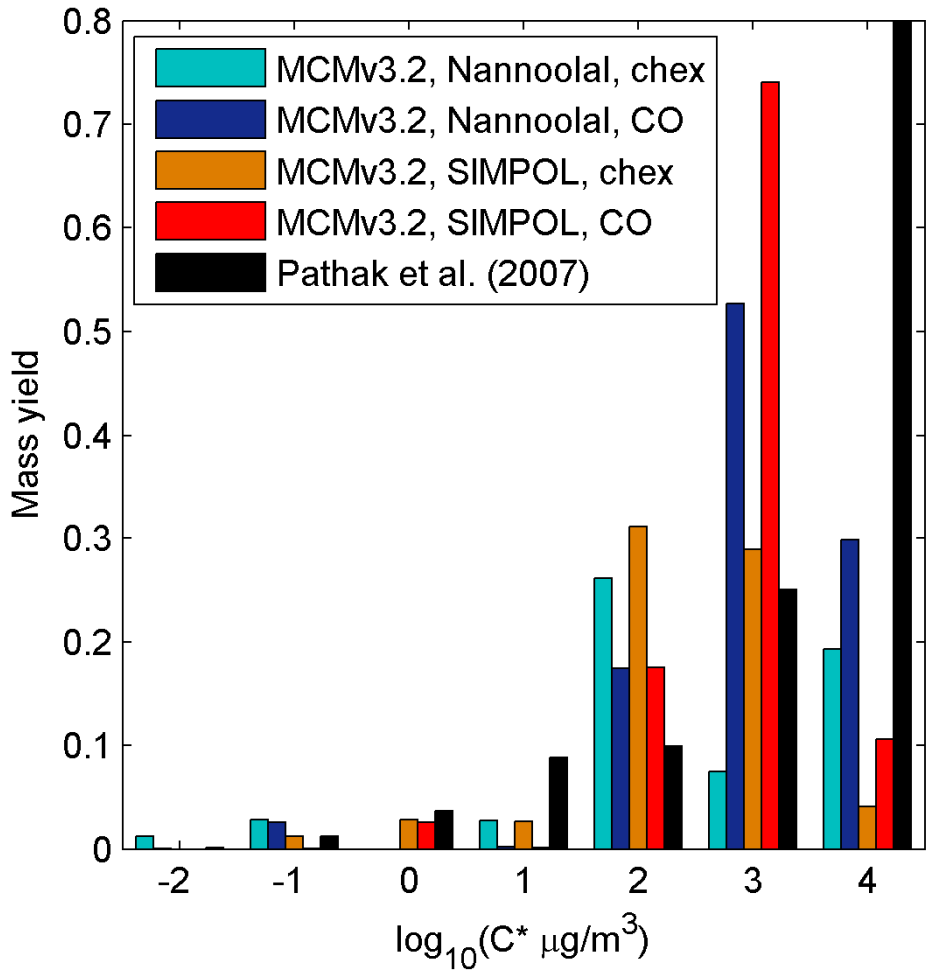

Figure S4. Derived VBS from the simulated α-pinene oxidation experiments from Na et al. (2007) with CO as OH scavenger, and from Vaden et al. (2011) with cyclohexane as OH scavenger. The VBS parameterizations were derived with the pure-liquid saturation vapour pressure method from Nannoolal et al. (2008) and SIMPOL (Pankow and Asher, 2008). Shown is also the experimentally derived VBS parameterization from Pathak et al. (2007). The influence from wall losses was not considered for these simulations.

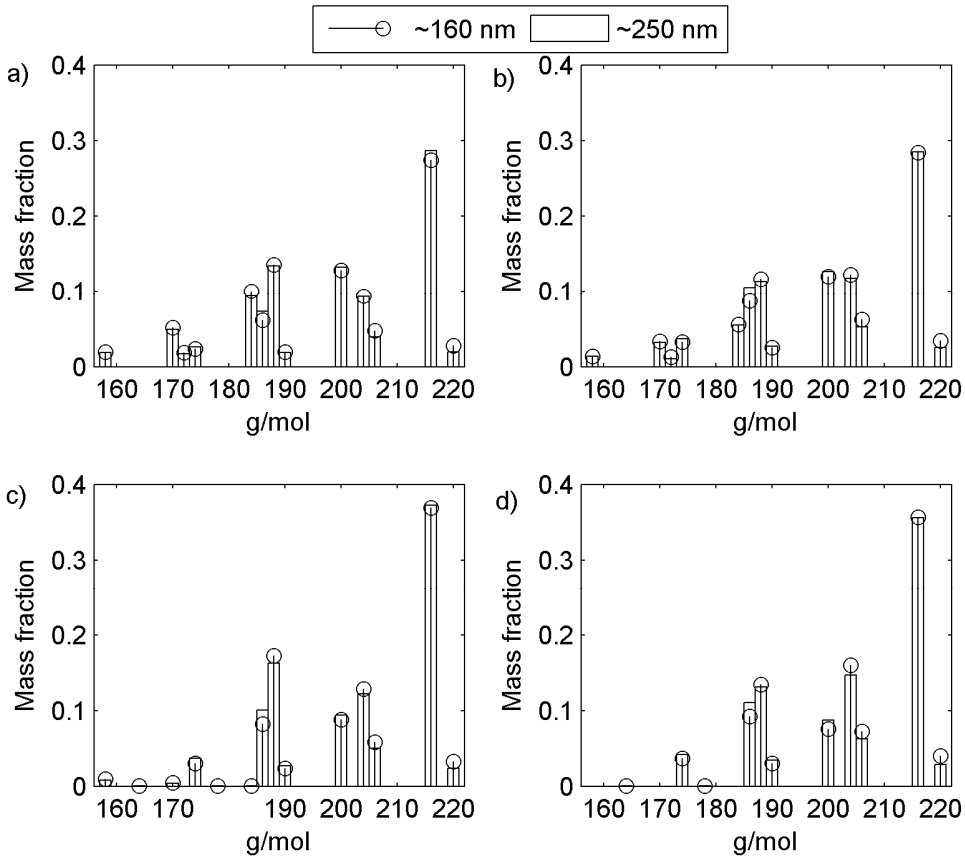

Figure S5. Modelled monomer mass spectrum of solid SOA particles formed by ozonolysis of α-pinene. (**a**) with the SIMPOL saturation vapour pressure method and no gas-wall partitioning, (**b**) with SIMPOL and gas-wall partitioning ($k_{g,w}^{*}$=1/2000 s^{-1} and $C_w / \left(M_w \gamma_{w,i}\right)$=100 μmol m^{-3}), (**c**) with the saturation vapour pressure method from Nannoolal et al. (2008) and no gas-wall partitioning and (**d**) the Nannoolal method and gas-wall partitioning (with SIMPOL and gas-wall partitioning ($k_{g,w}^{*}$=1/2000 s^{-1} and $C_w / \left(M_w \gamma_{w,i}\right)$=100 μmol m^{-3}). The low volatile MCMv3.2 oxidation products C922OOH and C813OOH have mass peaks at 220 and 206 g/mol, respectively.

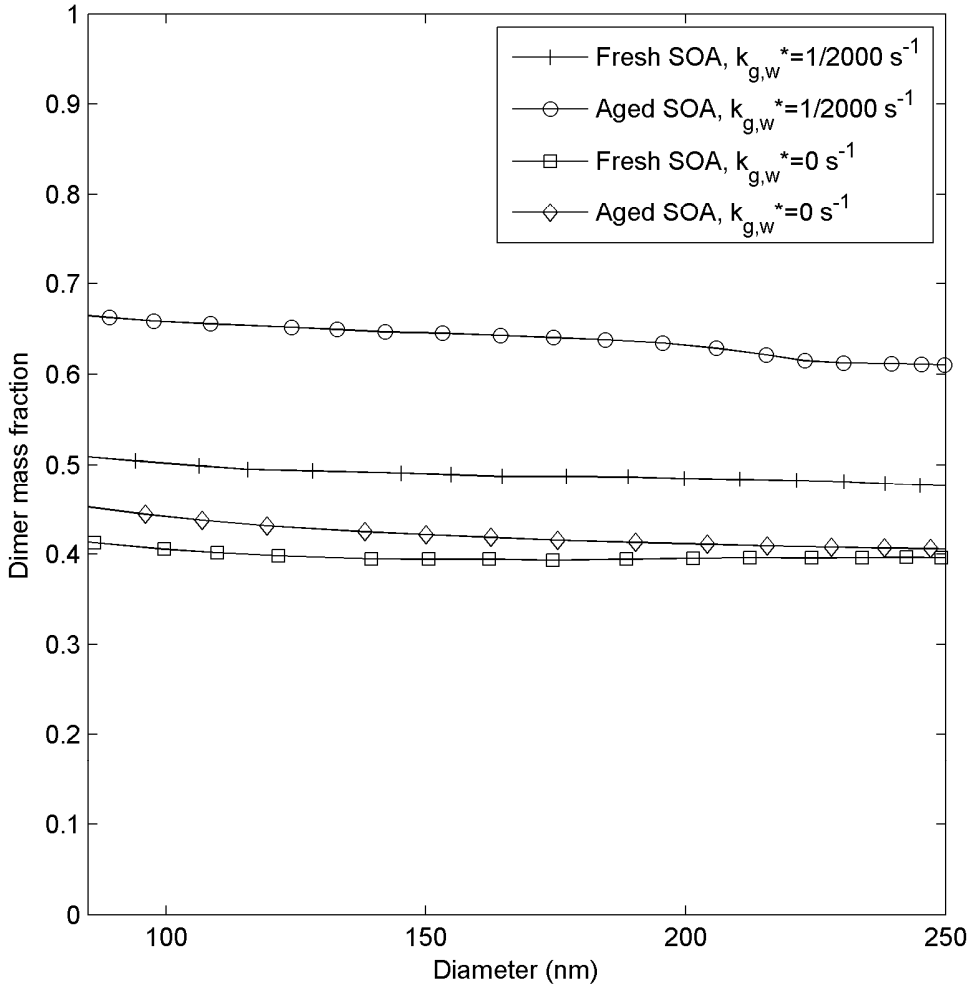

Figure S6. Modelled dimer mass fraction of fresh (1.5 hours) and aged (12 h) α-pinene SOA for different particle sizes. The results are from simulations with saturation vapour pressures calculated with SIMPOL, $k_{g,w}^{*}$=1/2000 s^{-1} or $k_{g,w}^{*}$=0 s^{-1}, $C_w / \left(M_w \gamma_{w,i}\right)$=100 μmol m^{-3}, $D_{0,\mathrm{monomer}}$ = 2x10^{-14} cm^2 s^{-1}, D_{dimer} = 2x10^{-16} cm^2 s^{-1}, k_f = 10^{-23} $molecules^{-1}$ cm^3 s^{-1}, k_d = 1/10 h^{-1} and no phase separation.

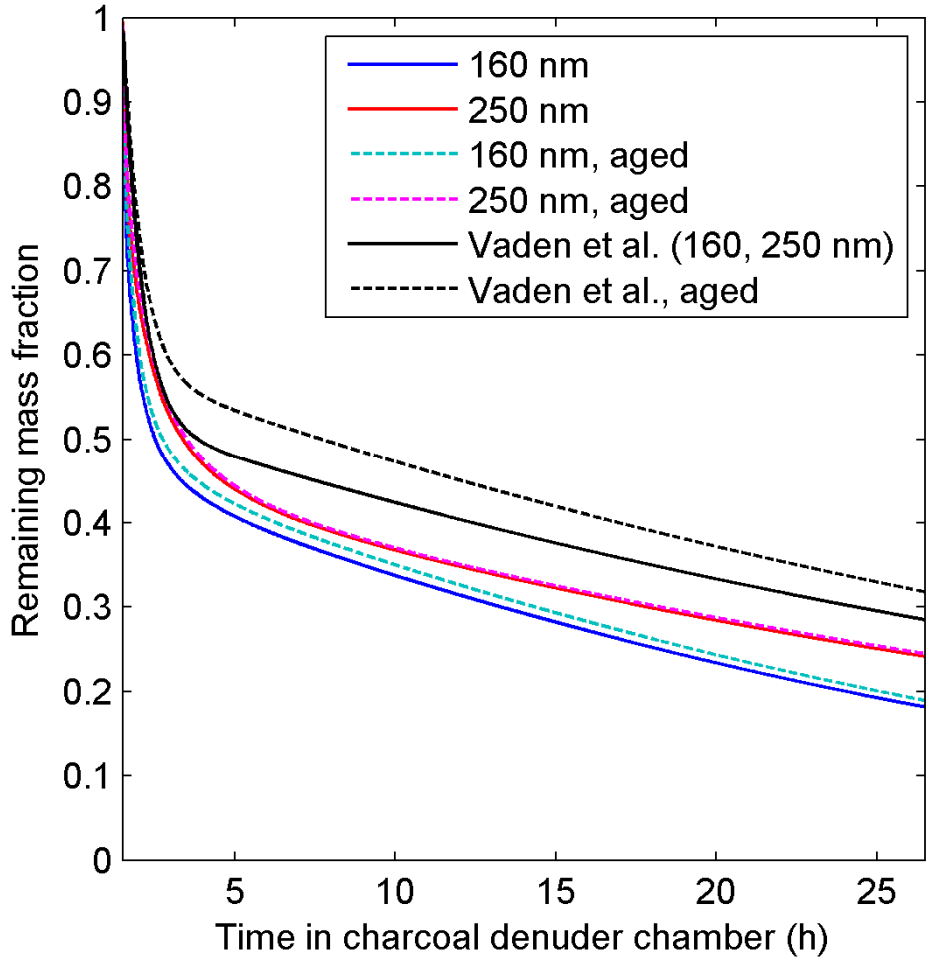

Figure S7. Measured (Vaden et al., 2011) and modelled evaporation losses for particles composed of ~40 % dimer and 60 % monomer SOA (see Fig. S6), prior to the introduction in the charcoal denuder chamber. The saturation vapour pressures were calculated with SIMPOL, $D_{0,\text{monomer}}$ = 2x10^{-14} cm^2 s^{-1}, D_{dimer} = 2x10^{-16} cm^2 s^{-1}, k_f = 10^{-23} molecules^{-1} cm^3 s^{-1}, k_d = 1/10 h^{-1}, no phase separation and a $k_{g,w}^*$ = 0 s^{-1}. The results are given both for fresh and aged particles with a diameter of ~160 nm and ~250 nm, respectively.

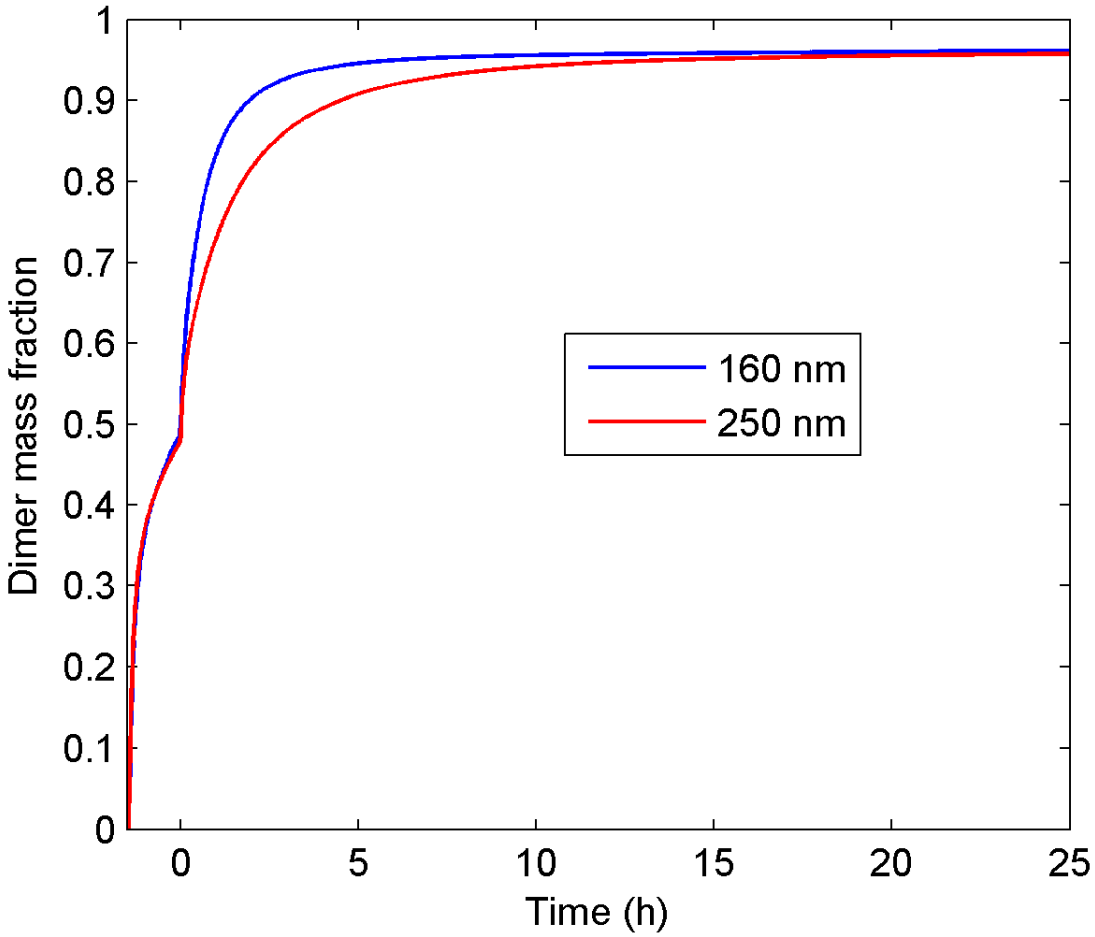

Figure S8. Modelled dimer mass fraction of particles with a diameter of ~160 and ~250 nm, prior to the introduction in the charcoal denuder chamber (0 h). The results are from a simulation with saturation vapour pressures from SIMPOL, $D_{0,\text{monomer}}$ = 2x10^{-14} cm^2 s^{-1}, D_{dimer} = 2x10^{-16} cm^2 s^{-1}, k_f = 10^{-23} molecules^{-1} cm^3 s^{-1}, k_d = 1/10 h^{-1}, no phase separation and a $k_{g,w}^*$ = 1/2000 s^{-1}.

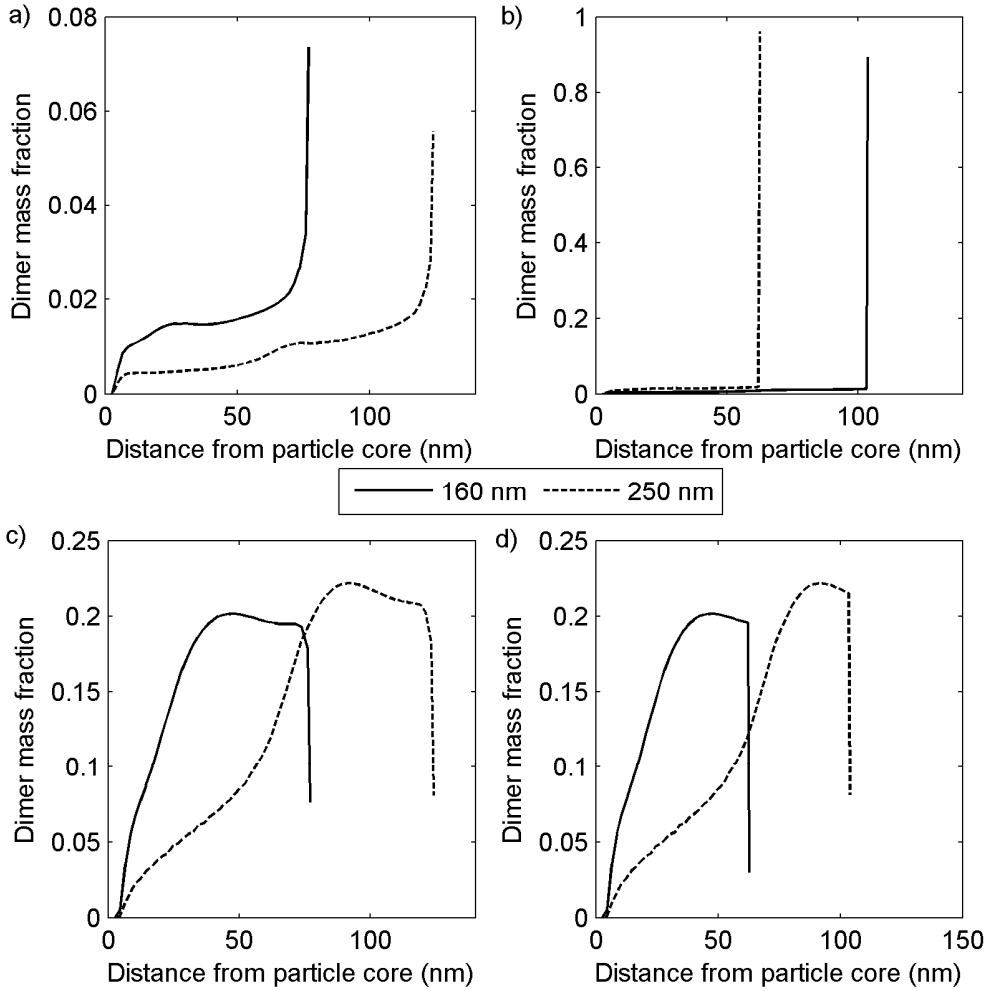

Figure S9. Modelled mass fractions of long-lived (**a**-**b**) and short-lived dimers (**c**-**d**), at different distances from the particle core. The results are given both for particles with a diameter of ~160 and 250 nm, before evaporation. Figure **a** and **c** shows the composition of the particles before they are introduced into the evaporation chamber while **b** and **d** gives the dimer content after 2 hours in the evaporation chamber. In the model $D_{0,monomer}$ was 5×10^{-17} cm^2 s^{-1} and $D_{oligomer}$ was 0 cm^2 s^{-1}. The saturation vapour pressures were calculated with SIMPOL and $k_{g,w}^*$ was equal to 1/1000 s^{-1}.

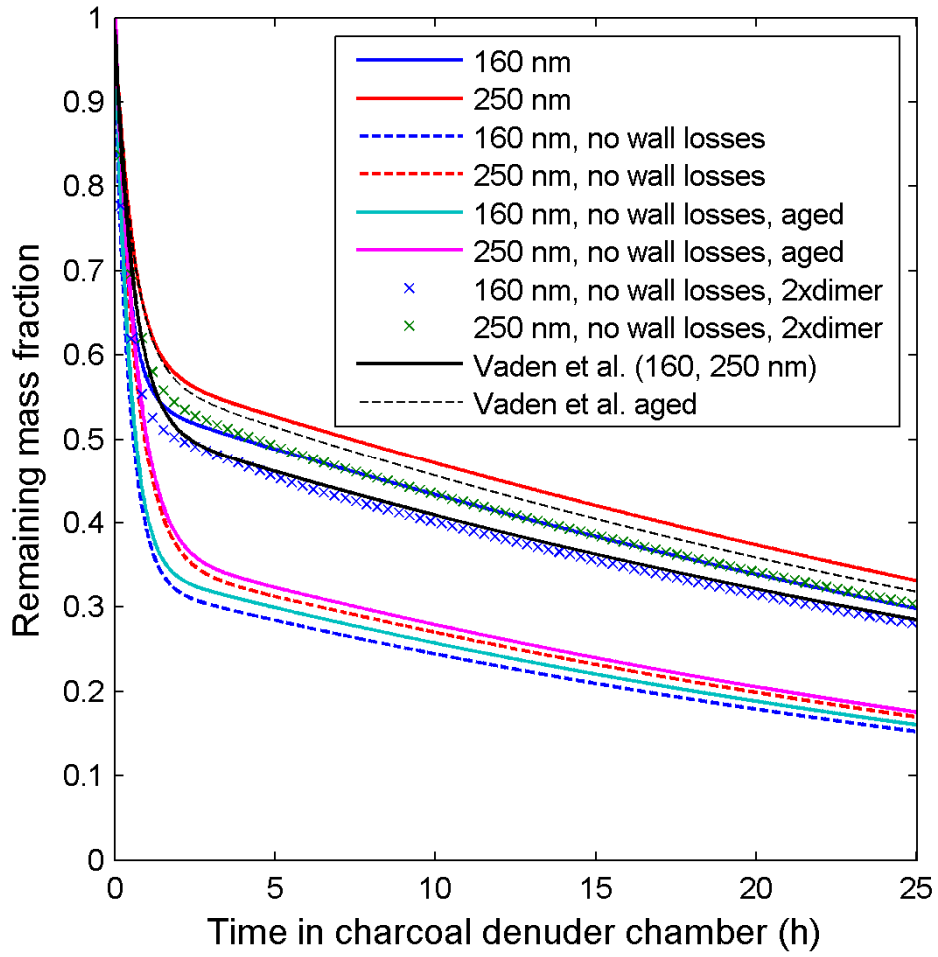

Figure S10. Measured (Vaden et al., 2011) and modelled evaporation loss rates for semi-solid tar like particles ($D_{0,monomer}$=5x10^{-17} cm^2 s^{-1} and $D_{oligomer}$=0 cm^2 s^{-1}). The saturation vapour pressures were calculated with SIMPOL and $k_{g,w}^*$ was equal to 1/1000 s^{-1} or 0 s^{-1} (no wall losses). Without wall losses fresh (1.5 h) and aged (12 h) particles have nearly identical evaporation rates. For these simulations the long-lived dimer content in the surface-bulk layer is substantially lower than for the simulations with wall losses. Thus, more monomer SOA evaporates during the first evaporation stage. However, if we double the long-lived dimer content and run the model without wall losses, the model results agree very well with the observations. The only difference is that the small particles lose ~3 % more mass during the first evaporation stage.

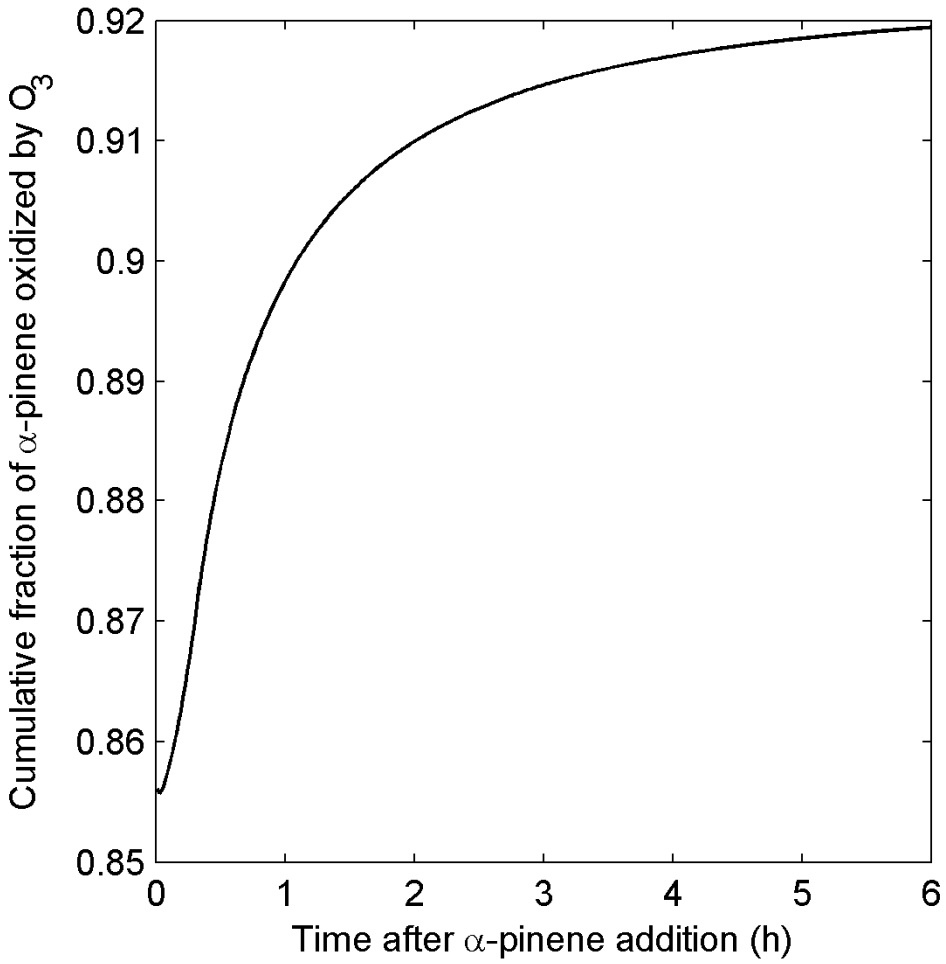

Figure S11. Cumulative fraction of α-pinene oxidized by O_3 for the modelled experiments from Na et al. (2007).

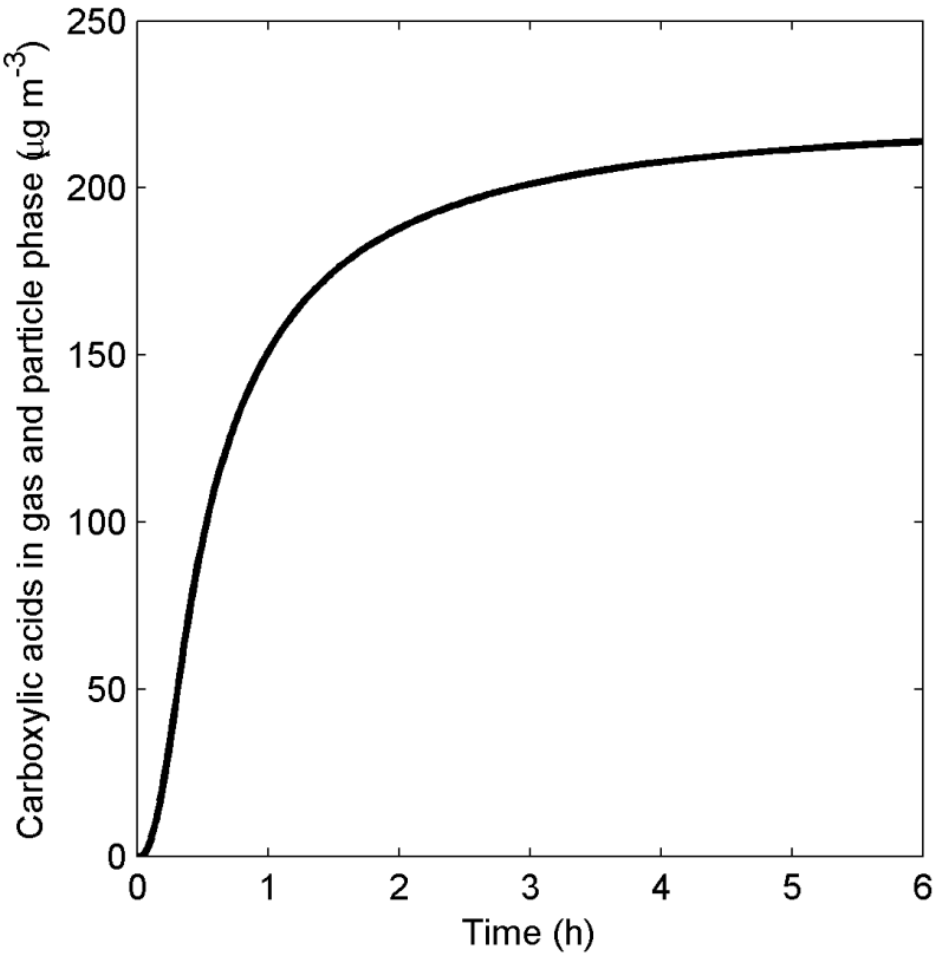

Figure S12. Modelled total carboxylic acids concentration in the gas and particle phase during the α-pinene oxidation experiments from Na et al. (2007).

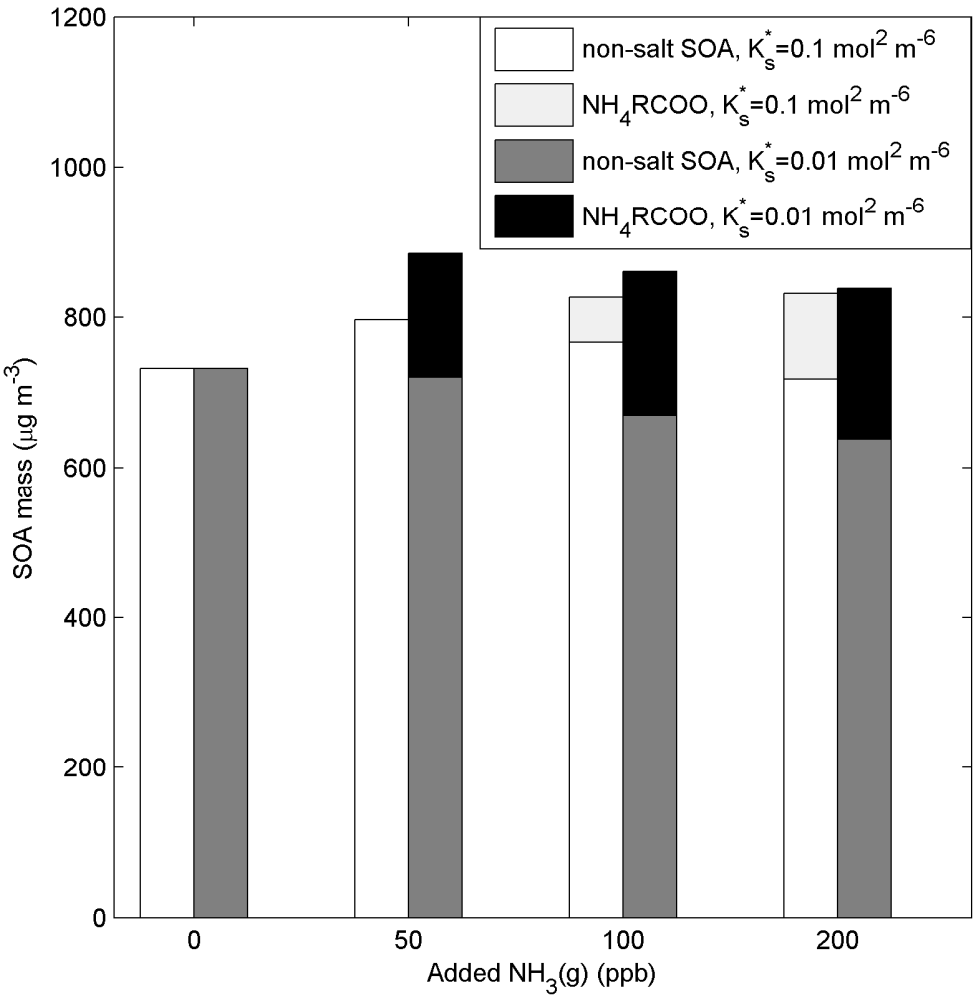

Figure S13. Comparison of modelled SOA mass formation with an effective solubility product (K_s^*) of 0.01 or 0.1 mol^2 m^{-6} for the organic salts of carboxylic acids and ammonium (NH_4RCOO). The total aerosol mass is divided into the fraction composed of non-salt SOA and NH_4RCOO.

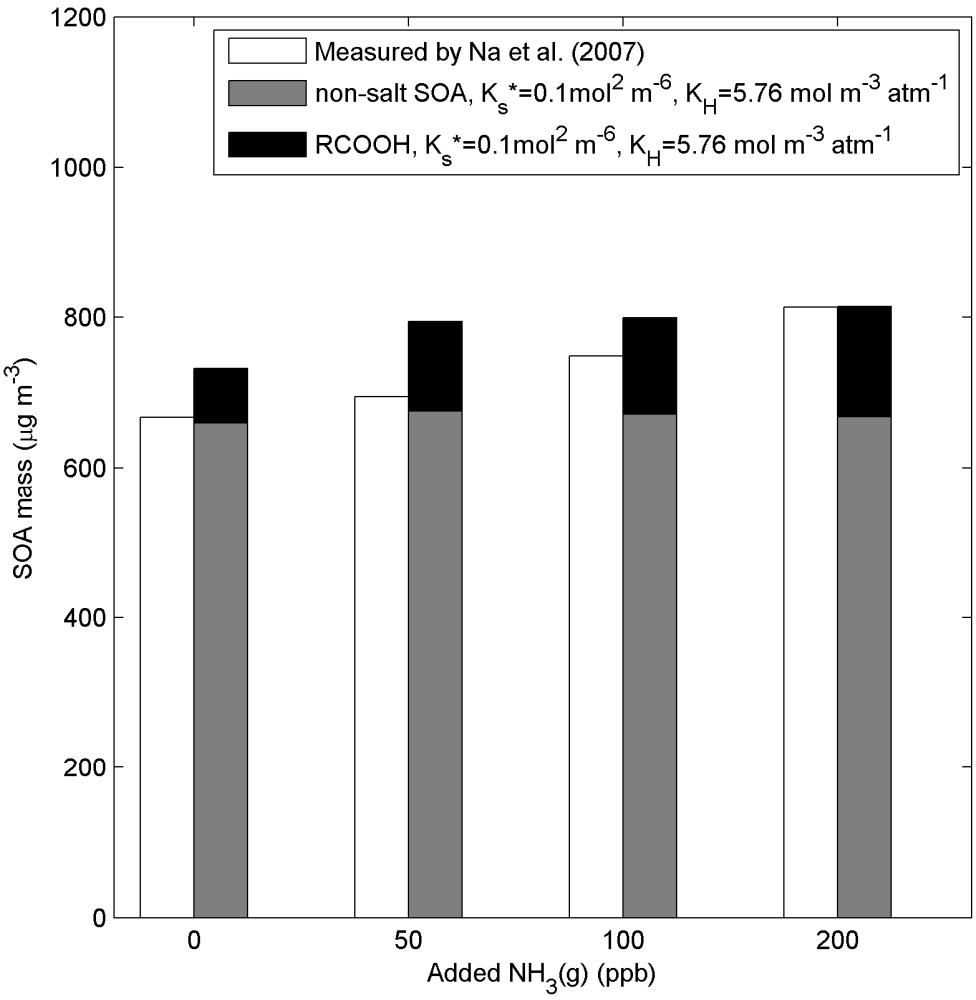

Figure S14. Comparison of measured and modelled SOA mass formation. The modelled mass is divided into the SOA fraction composed of carboxylic acids (RCOOH) and other SOA monomers. The model simulations were performed with an effective solubility product (K_s^*) of 0.1 mol^2 m^{-6} for the organic salts of carboxylic acids and ammonium (NH_4RCOO), and a Henry's law coefficients of NH_3 (K_H) which is 10 times lower than for aqueous solutions. No NH_4RCOO was formed in the modelled particles.

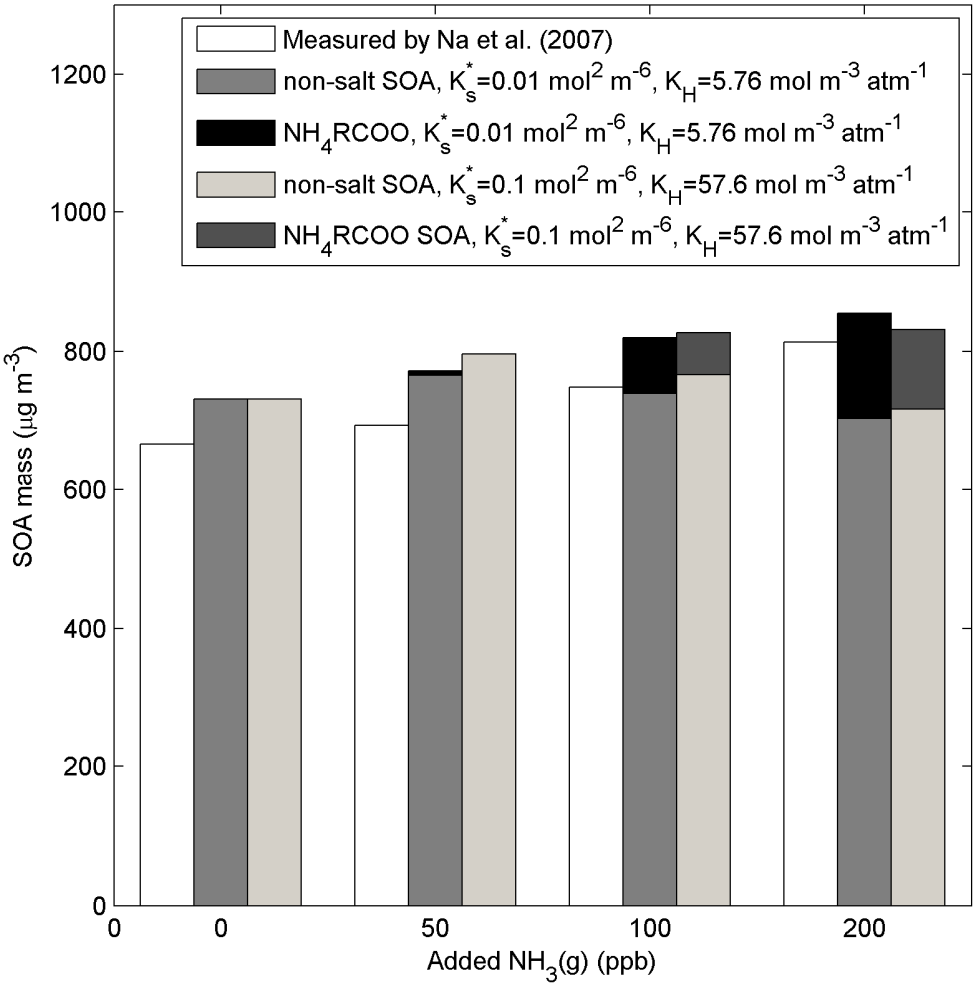

Figure S15. Comparison of modelled and measured SOA mass formation. The model results are from simulations with K_s^* = 0.01 mol^2 m^{-6} and 10 times lower Henry's law coefficients of NH_3 (K_H) than in water, and K_s^* = 0.1 mol^2 m^{-6} and the Henry's law coefficients for NH_3 dissolution in water. The total aerosol mass is divided into the fraction composed of non-salt SOA and NH_4RCOO.

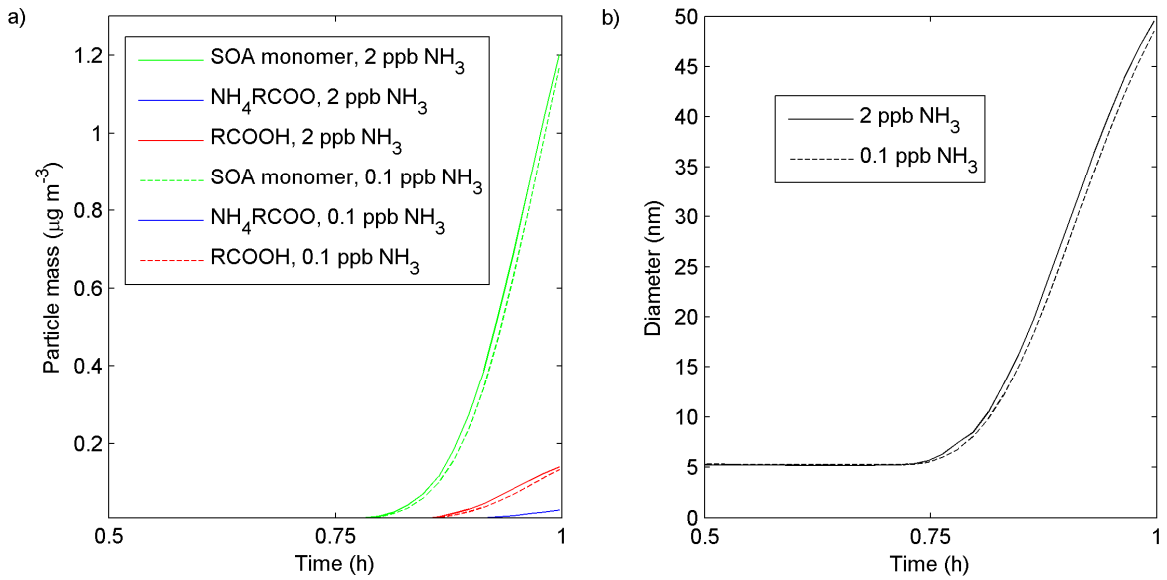

Figure S16. Modelled (**a**) total SOA monomer, NH_4RCOO and RCOOH concentrations and (**b**) particle diameter growth, for simulations with initially ~50 ppb α-pinene, ~200 ppb O_3, ~200 ppm CO and 2 or 0.1 ppb NH_3. The simulations were performed with only one particle size, which initially is 5 nm in diameter.

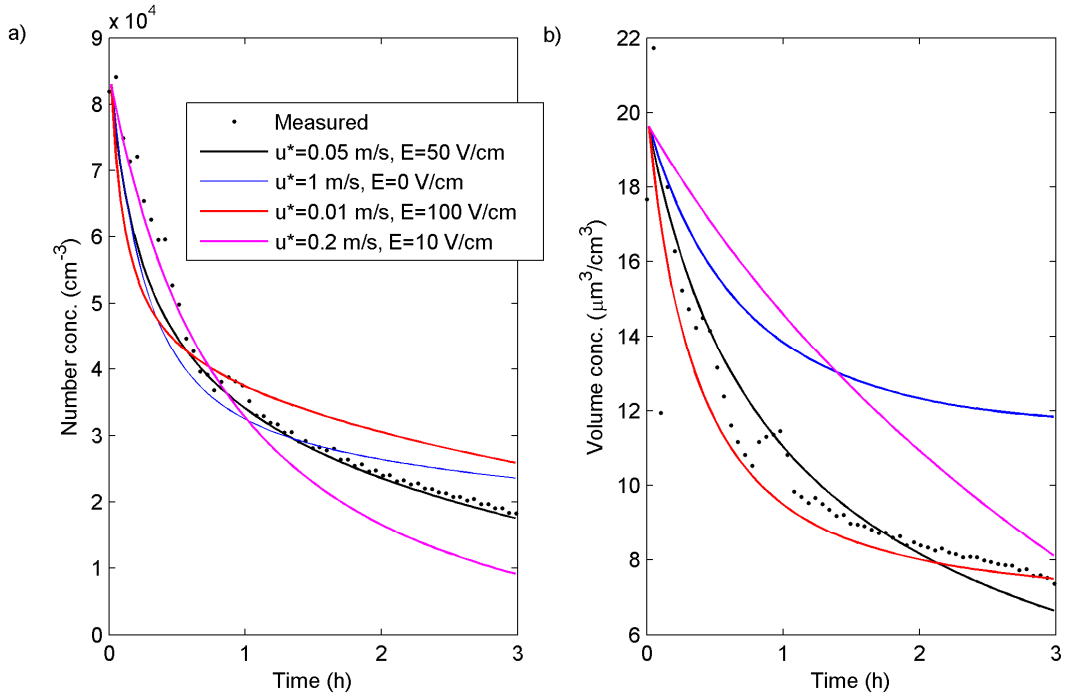

Figure S17. Modelled and measured (**a**) particle number- and (**b**) particle volume concentration of ammonium sulphate seed aerosol particles in a Teflon smog chamber. The initial chamber volume was 6 m^3 and during the experiment it decreases with ~0.8 m^3 h^{-1}. The mean electrical field strength ($\bar{E}$) and the friction velocity (u^*) was used as model fitting parameters. The overall best agreement between the model and measured particle number and particle volume concentration losses are found when using a u^* of ~0.05 m s^{-1} and a $\bar{E}$ of ~50 V cm^{-1}.

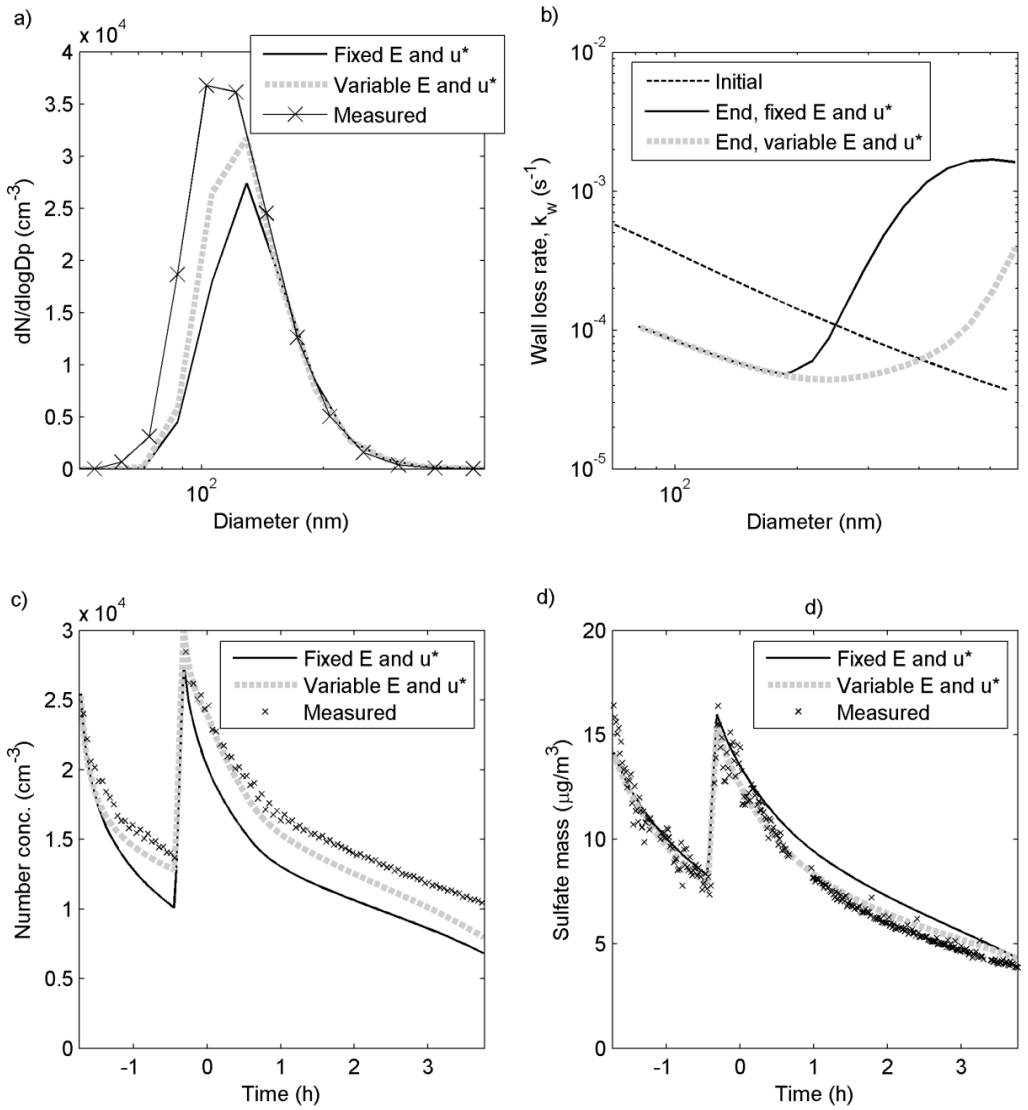

Figure S18. Modelled and measured a) particle number size distribution at the end of the *m*-xylene experiment, b) initial and final effective wall deposition loss rates (modelled), c) number concentration and d) sulphate seed aerosol mass concentration. The model results are from a simulation with a fixed $\overline{E}_t$ of 50 V cm^{-1} and a u^* of 0.05 m s^{-1} or variable $\overline{E}_t$ calculated with Eq. (30) and u^* = 0.01 m s^{-1} before the UV-lights are turned on and u^* = 0.05 m s^{-1} after the UV-lights are turned on.

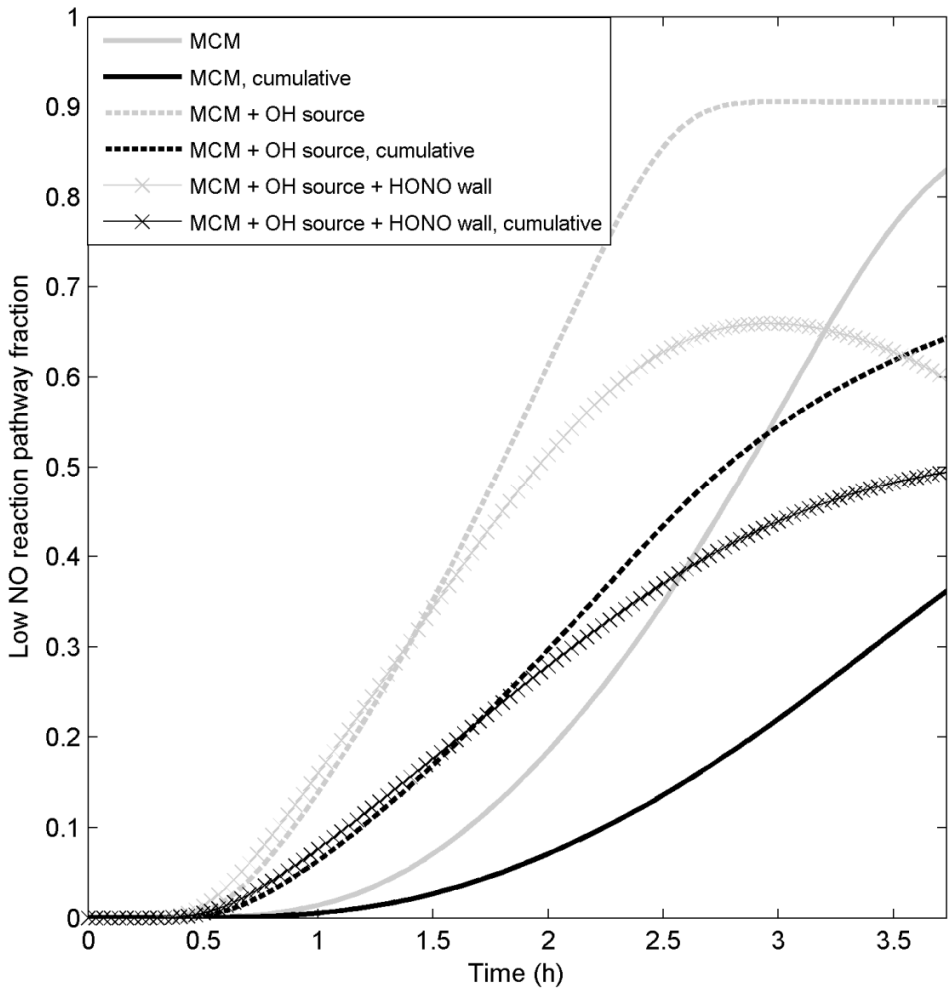

Figure S19. Modelled current time step and cumulative fraction of the *m*-xylene first generation RO_2 products that react (have reacted) with HO_2 instead of NO. The results are given for simulations with the original MCMv3.2 gas phase chemistry, with MCMv3.2 gas phase chemistry and an artificial OH source of 10^8 cm^3 s^{-1}, and with MCMv3.2 gas phase chemistry, the artificial OH source and wall emissions of HONO.

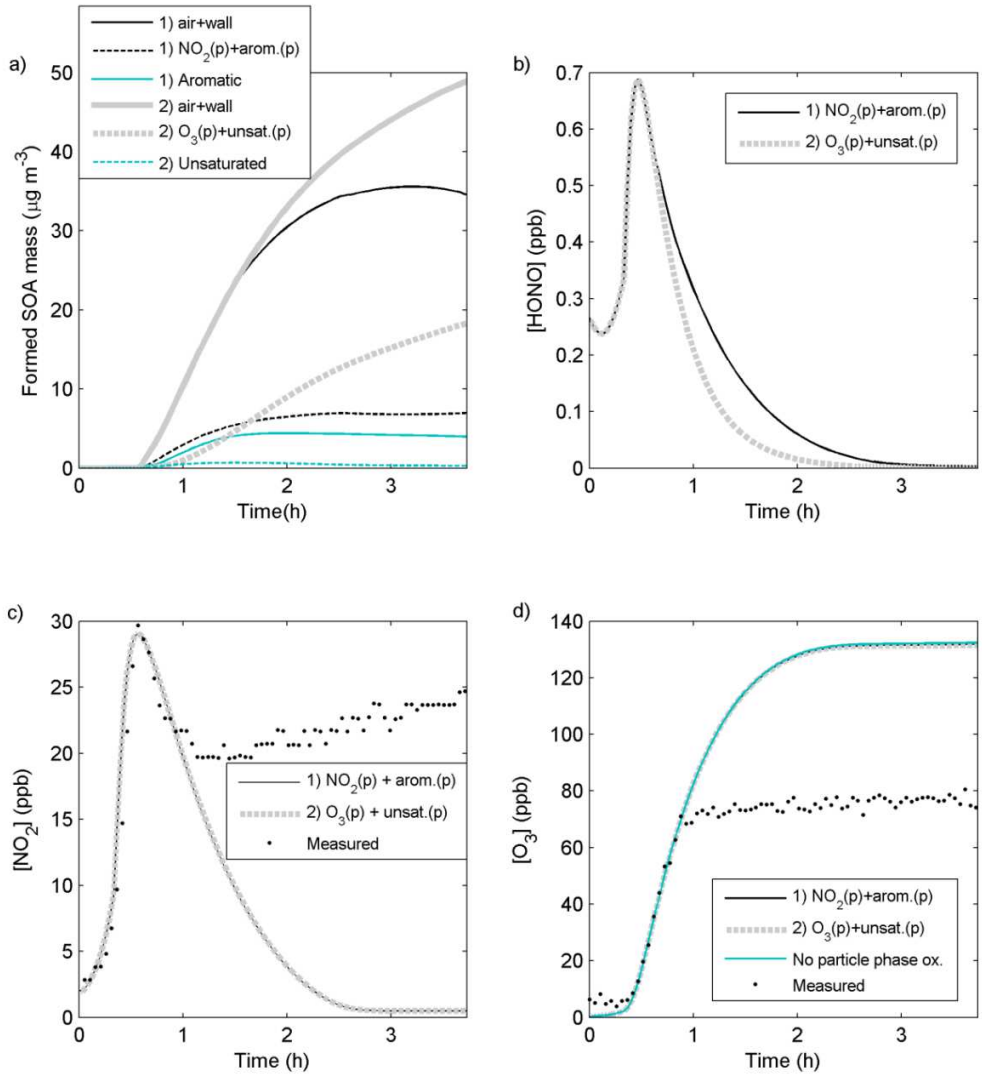

Figure S20. Results from simulations of the *m*-xylene oxidation experiment by Nordin et al. (2013) when considering 1) HONO formation from heterogeneous reactions (k_{NO_2} =10^{-15} cm^{-3} s^{-1} and D_{0,NO_2} =10^{-7} cm^2 s^{-1}) or 2) heterogeneous reactions of O_3 (k_{O_3} =10^{-16} cm^{-3} s^{-1} and D_{0,O_3} =10^{-7} cm^2 s^{-1}). For simulation Nr. 1 Fig. a shows the total SOA mass (air + wall), SOA mass of formed oxidation products from the reaction between the aromatic compounds and NO_2, and the remaining non reacted aromatic SOA mass. For simulation Nr. 2 Fig. a shows the total SOA mass, SOA mass of formed oxidation products from the heterogeneous O_3 reactions, and the remaining non reacted unsaturated organic SOA mass. Figure b shows the modelled HONO concentration, c) the NO_2 concentration and d) the O_3 concentration. In Fig. d we also included the results from a simulation without heterogeneous oxidation reactions.

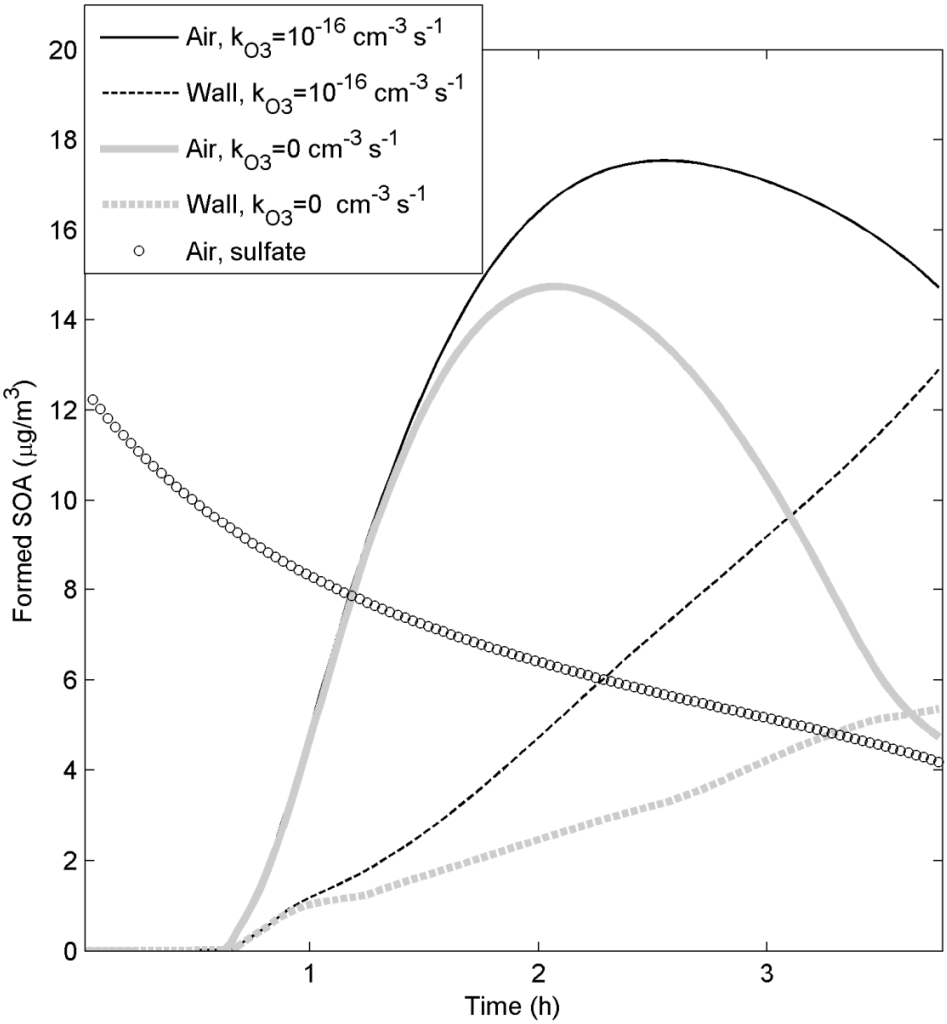

Figure S21. Modelled SOA mass formation in the air and on the wall deposited particles during the *m*-xylene oxidation experiment by Nordin et al. (2013). The results are from simulations with a laminar layer width (Δx) of 1.0 cm adjacent to the chamber walls and a first order loss rate from the near wall gas phase to the walls ($k_{g,w}$) of 1/6 s^{-1}. ADCHAM was either run without or with heterogeneous reactions between O_3 and the unsaturated organic compounds ($k_{O_3}=10^{-16}$ cm^{-3} s^{-1} and $D_{0,O_3}=10^{-8}$ cm^2 s^{-1}).

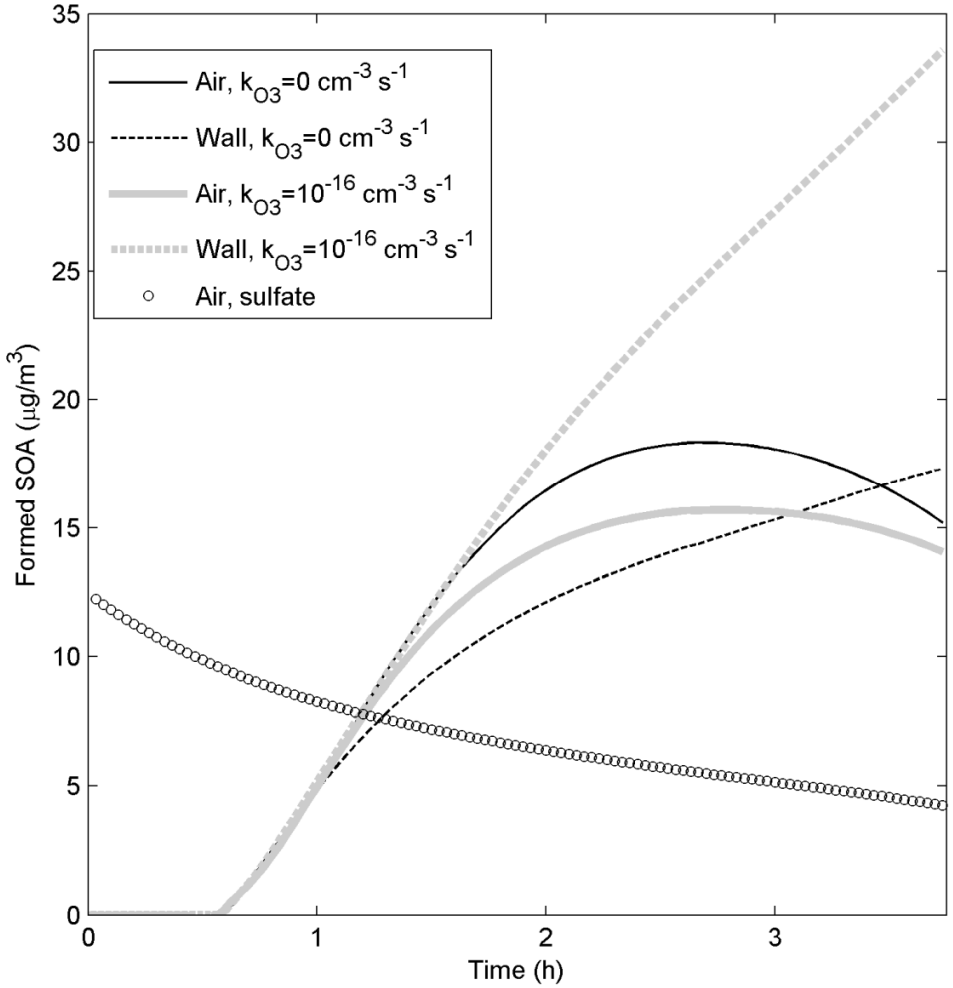

Figure S22. Modelled SOA mass formation in the air and on the wall deposited particles during the *m*-xylene oxidation experiment by Nordin et al. (2013). The results are from simulations with a laminar layer width (Δx) of 0.1 cm adjacent to the chamber walls and a first order loss rate from the near wall gas phase to the walls ($k_{g,w}$) of 1/20 s^{-1}. ADCHAM was either run without or with heterogeneous reactions between O_3 and the unsaturated organic compounds (k_{O_3} =10^{-16} cm^{-3} s^{-1} and D_{0,O_3} =10^{-8} cm^2 s^{-1}).

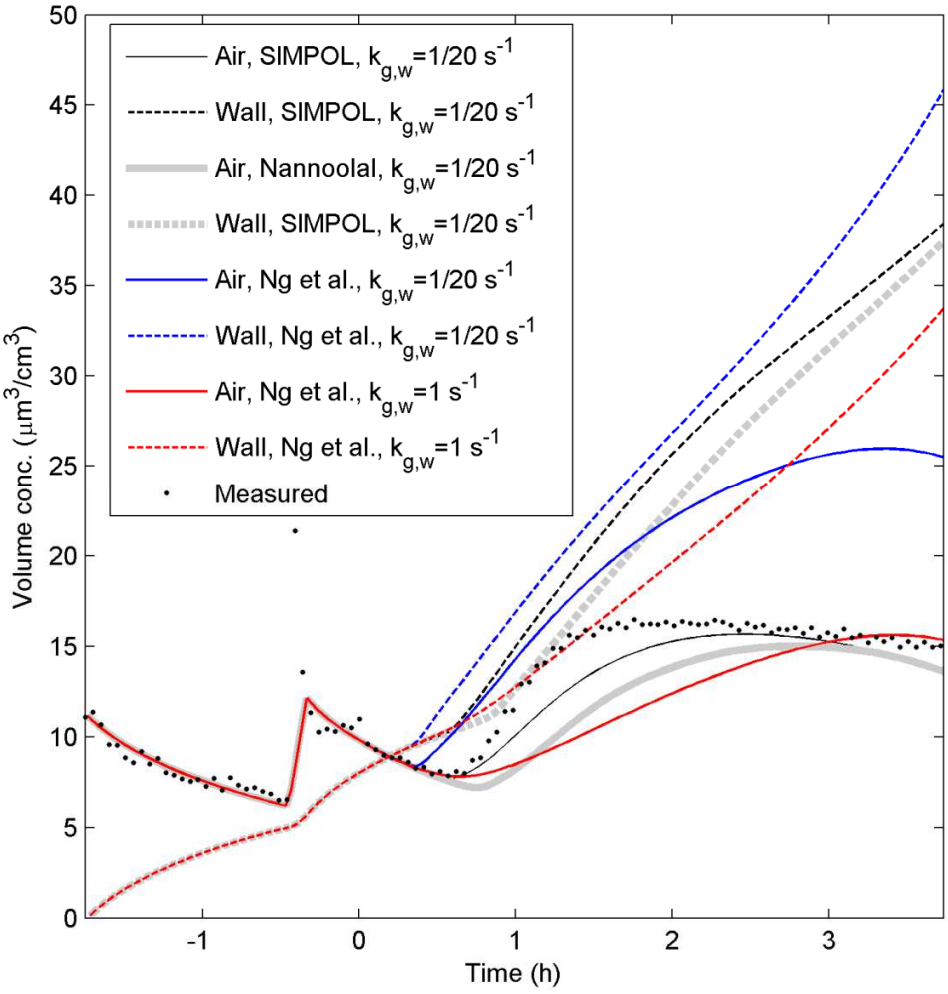

Figure S23. Modelled and measured volume concentrations (seed aerosol + SOA coating) during the *m*-xylene oxidation experiment by Nordin et al. (2013). The model results are from siumations with the SIMPOL (Pankow and Asher, 2008), Nannoolal et al. (2008) vapour pressure method or the semi-empirical parameterizations from Ng et al. (2007). The figure shows both the modelled particle volume concentrations in the air and on the walls.

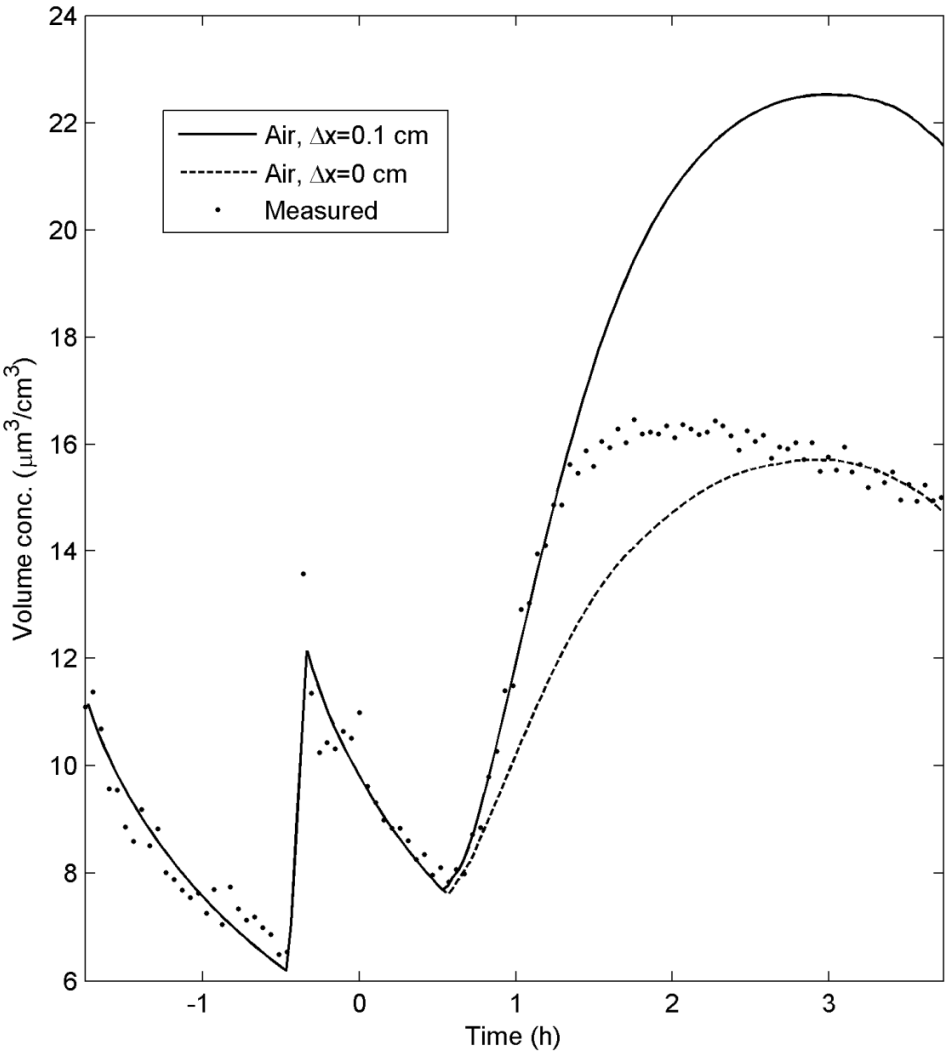

Figure S24. Modelled and measured particle volume concentrations in the air from the *m*-xylene oxidation experiment by Nordin et al. (2013). The model results are from simulations with a laminar layer of 0 or 0.1 cm adjacent to the chamber walls and without uptake of organic compounds directly onto the Teflon walls.